Biosensors and Bioelectronics 91 (2017) 857–862

Contents lists available at ScienceDirect

Biosensors and Bioelectronics

journal homepage: www.elsevier.com/locate/bios

Monitoring of microbial cell viability using nanostructured electrodes modified with Graphene/Alumina nanocomposite

Rabeay Y.A. Hassan[a,c,*], Moataz M. Mekawy[d], Pankaj Ramnani[a], Ashok Mulchandani[a,b]

[a] Department of Chemical and Environmental Engineering, University of California, Riverside, CA 92521, United States
[b] Materials Science and Engineering Program, University of California, Riverside, CA 92521, United States
[c] Microanalysis Lab, Applied Organic Chemistry Department, National Research Centre (NRC), El Bohouth st., Dokki, 12622 Giza, Egypt
[d] National Institute for Materials Science, 1 Chome-2-1 Sengen, Tsukuba, Ibaraki Prefecture 305-0047, Japan

ARTICLE INFO

Keywords:
Nano-microbial sensors
Cell viability measurement
Electrochemical assay
Modified electrode
Aluminum oxide
Graphene oxide
Nanocomposite

ABSTRACT

Microbial infections are rapidly increasing; however most of the existing microbiological and molecular detection methods are time consuming and/or cannot differentiate between the viable and dead cells which may overestimate the risk of infections. Therefore, a bioelectrochemical sensing platform with a high potential to the microbial-electrode interactions was designed based on decorated graphene oxide (GO) sheet with alumina (Al_2O_3) nanocrystals. GO-Al_2O_3 nanocomposite was synthesized using self-assembly of GO and Al_2O_3 and characterized using the scanning electron microscopy (SEM), transmission electron microscopy (TEM), x-ray diffraction (XRD), Raman-spectroscopy, electrochemical impedance spectroscopy (EIS) and cyclic voltammetry (CV). Enhancement of electrocatalytic activity of the composite-modified electrode was demonstrated. Thus, using the GO-Al_2O_3 nanocomposite modified electrode, the cell viability was determined by monitoring the bioelectrochemical response of the living microbial cells (bacteria and yeast) upon stimulation with carbon source. The bioelectrochemical assay was optimized to obtain high sensitivity and the method was applied to monitor cell viability and screen susceptibility of metabolically active cells (*E. coli, B. subtilis, Enterococcus, P. aeruginosa and Salmonella typhi*) to antibiotics such as ampicillin and kanamycin. Therefore, the developed assay is suitable for cell proliferation and cytotoxicity testing.

1. Introduction

Infectious diseases are a major cause of human mortality in many developing countries due to the presence of pathogenic organisms as biological contaminants in daily life (Chalenko et al., 2012). Thus, an early and rapid identification of microbial infection is necessary to provide efficient treatment; which still remains a challenge. To date, the available diagnostic tools primarily rely on microbiological assays, such as cell counting, selective growth, and microscopic examination (Spiegelman et al., 2005). However, these techniques are time-consuming and lack sensitivity and selectivity, especially for complex matrices. Consequently, molecular biological methods (e.g. PCR and ELISA) are used for detection of microbes. However, the inability to differentiate between viable and dead cells is a serious limitation of these techniques (Byrne et al., 2009; Lim et al., 2005; von Wintzingerode et al., 1997).

Recently, bioelectrochemical detections of living microorganisms by using microbial electrochemical systems (MES) have been exploited for the rapid assessment of microbial activities (Carmona-Martinez et al., 2011; Hassan and Bilitewski, 2013; Nishio et al., 2013; Park et al., 2008; Yoon et al., 2007), as well as for microbial fuel cells (Logan, 2009). In MES, electrochemically active organism transfer extracellular electrons to a terminal electron acceptor (e.g. electrode) to generate electrical current which reflects the metabolic activity of the target organism (Heiskanen et al., 2013).

There are two extracellular electron transfer concepts; namely, direct electron transfer (DET) and mediated electron transfer (MET). In the DET process, a physical contact of a redox active microbial moiety (Yang et al., 2012), including redox proteins like cytochromes or bacterial nanowires (Gorby et al., 2006; Reguera et al., 2005), with the electrode surface have been recognized. On the other hand, in the MET process the microbe-electrode communication is mediated by exogenous redox mediators (either natural i.e. secretion of electroactive molecules by the target organism(s) or artificial using artificial electron shuttles) (Marsili et al., 2008; Rabaey et al., 2005; Schroder, 2007).

However, due to the cytotoxicity and interference, the artificial redox mediators are major drawbacks of these techniques.

Thus, development of new electrode materials is a critical factor to

* Corresponding author at: Microanalysis Lab, Applied Organic Chemistry Department, National Research Centre (NRC), El Bohouth st., Dokki, 12622 Giza, Egypt.
E-mail address: rabeayy@gmail.com (R.Y.A. Hassan).

http://dx.doi.org/10.1016/j.bios.2017.01.060
Received 24 November 2016; Received in revised form 22 January 2017; Accepted 25 January 2017
Available online 26 January 2017
0956-5663/

enable direct detection of living cell activity and avoid the use of chemical redox mediators. To this end, smart conducting materials that can wire the microbial cells with the electrode surface are suggested. Taking into account the interesting electron transfer properties of various nanomaterials, e.g. nanoparticles, nanowires (NWs), carbon nanotubes (CNTs) and graphene (Esfandiari Baghbamidi et al., 2012; Tian and Lieber, 2013; Yuan et al., 2011; Zhao et al., 2012), it is hypothesized that these materials would be able to facilitate redox reaction(s) between biomolecules and electrode surfaces and thus could provide suitable candidate platforms for direct electrochemical detections.

One material that is receiving a great deal of interest in recent years is nanocomposites of graphene oxide with metal oxide producing future promising platforms for biosensors, fuel cells and supercapacitors applications. Wang et al., (2009) reported the use of graphene oxide/TiO_2 nanocomposite for investigation of Li-ion insertion properties and demonstrated faster Li-ion insertion/extraction kinetics and higher specific capacity in the presence of a percolated graphene network embedded into the metal oxide electrodes. Chen et al. (2010), reported about the synthesis of graphene oxide/MnO_2 nanocomposite as an electrode material for supercapacitor application. Recently, we have reported about the non-enzymatic H_2O_2 detection using GO/ZnO nanocomposite.

Thus, the concern of this work is to fabricate a nano-structured-microbial electrochemical platform for the direct monitoring of viable microorganisms. To achieve this goal, a biosensing platform with a high potential for the microbial-electrode interactions based on graphene oxide (GO) sheet decorated with alumina (Al_2O_3) nanocrystals was synthesized, fully characterized (using physical and electrochemical techniques) and used in a chemically-modified electrode (CME) for determining metabolic pathway activity of microbial cultures to monitor viable cells and response to antibiotics.

2. Experimental details

2.1. Materials

Graphite flakes, sulfuric acid (H_2SO_4), potassium permanganate ($KMnO_4$), Alumina (Al_2O_3), phosphoric acid (H_3PO_4), hydrochloric acid (HCl) and ethanol were purchased from Sigma-Aldrich.

2.2. Synthesis of graphene oxide (GO)

GO was synthesized according to the modified Hummer's method (Marcano et al., 2010). Briefly, 75 ml of a mixture of concentrated H_2SO_4/H_3PO_4 (4:1 vol ratio) was added to 3.0g of purified natural graphite in a flask, followed by dropwise addition of 10.5 ml $KMnO_4$ while keeping the temperature at 4 °C using ice bath. The temperature was slowly increased to 60 °C and the mixture was continuously stirred for 12 h. One hundred ml of deionized water was added to the mixture, followed by addition of 5 ml of 30% H_2O_2. A precipitate of GO was collected and washed thoroughly with 500 ml of 1.0 M HCl using vacuum filtration, followed by washing with ethanol and deionized water. Colloidal GO was collected by centrifugation at 6000 rpm for 30 min, followed by drying at 80 °C.

2.3. Synthesis of Al_2O_3-GO composite

Commercially available α-Al_2O_3 powder (99.99% purity, average particle size: 200 nm) was used in this study. One gram of Al_2O_3 was sonicated for 1 h in 100 ml of deionized water (pH 4.1). 100 mg of GO was added to the suspension under vigorous stirring for 30 min. The resulting GO-Al_2O_3 nanocomposite particles, which had a light brownish color, were separated from the solution using vacuum filtration, followed by overnight drying at 100 °C.

2.4. Physical characterization of Al_2O_3-GO composite

The morphology, size and crystallinity of the GO-Al_2O_3 nanocomposite particles were characterized using scanning electron microscopy (JEOL JSM 6500 F), transmission electron microscopy (JEOL JEM 2100 F), Raman spectroscopy (Horiba LabRam/AIST-NT AFM microscope) and x-ray diffraction (Bruker Advance D8). For SEM, the GO-Al_2O_3 powder was sonicated in acetone to ensure the particles were well dispersed followed by drop casting deposition on a C-tape and kept for drying before imaging process. For TEM, the dispersed GO-Al_2O_3 powder was drop-casted on high-resolution C-coated TEM grid and kept for drying before TEM imaging. For Raman spectroscopy the GO-Al_2O_3 composite powder was sonicated in acetone and drop casted on a Si/SiO_2 substrate and the Raman spectra was obtained using 532 nm excitation source at a low power of 2 mW.

2.5. Electrode fabrication and electrochemical characterization

The GO-Al_2O_3 nanocomposite modified carbon paste electrodes (GO-Al_2O_3/CPE) were prepared by mixing 0.1 g of the GO-Al_2O_3 nanocomposite powder with 0.9 g of synthetic carbon powder and 0.3 ml paraffin oil using a mortar and pestle. The prepared paste was packed into the tip of the electrode assembly with a surface area of 0.5 cm^2. Electrode surface regeneration was performed by polishing with a wet smooth filter paper until a shiny electrode surface was obtained.

Prior to microbial electrochemical measurements, the working electrode was electrochemically activated in phosphate buffer solution (0.1 M, pH 7.0) by repeating 10 cyclic scans from −0.2 to +1.0 V at a scan rate of 50 mV/s. For measuring bioelectrochemical signals the cells were first incubated with 10 g/l of carbon sources for 3 h followed by addition of aliquots from the metabolically active cell suspension into the electrochemical cell and finally recording the cyclic voltammograms in the potential range from −0.2 to +1.0 V at scan rate of 50 mV/s without stirring at room temperature. All potentials are referred to Ag/AgCl/3.0 M KCl reference electrode.

2.6. Microbial cultivation and metabolic activation

Besides *Saccharomyces cerevisiae* as a yeast model organism, different bacterial strains such as *Escherichia coli, Bacillus subtilis, Enterococcus mutans, Pseudomonas aeruginosa* and *Salmonella typhi* were used in the study. Yeast and bacterial cells were cultivated overnight (around 17 h) in 250 ml flasks with 50 ml yeast extract peptone dextrose (YPD) and in Luria Broth (LB) medium at 30 °C and 37 °C, respectively. The cells were harvested by centrifugation (Eppendorf centrifuge 5804 R) at 5000 rpm for 5 min at room temperature and washed with phosphate buffer (pH 7) (Hassan and Bilitewski, 2011b, 2013). Different autoclaved solutions of phosphate buffer (0.1 M, pH 7) containing 10g/l of various carbon sources including glucose, sucrose, succinate, acetate, citrate and fructose were prepared. The metabolism of cells was stimulated by incubating the washed cells with the buffered carbon sources for 3 h at 37 °C in a shaker incubator.

2.7. Antibiotic treatment and assay validation

To investigate the response of cells to antibiotic treatment, a washed suspension of cells was incubated with 10 µg/ml and 50 µg/ml of ampicillin, kanamycin and amoxicillin for 3 h followed by measuring the bioelectrochemical response. In addition, the effect of antibiotics on cell viability was evaluated using the water-soluble tetrazolium (WST) assay where 50 µl of the WST reagent was added to 1 ml of a bacterial cell suspension in PBS (10 mM with pH 7.4) containing 10 g/l of glucose. The reagent was allowed to react for 30 min, before measuring the absorbance at 450 nm (Hassan and Bilitewski 2011a).

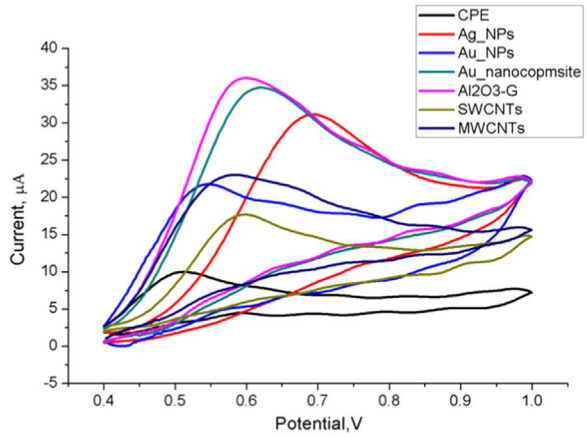

Fig. 1. Cyclic voltammograms of modified carbon paste electrode with 10% of each of nanomaterials, in 0.1 M PBS (pH 7.4) with 0.3 mM NADH at a scan rate of 50 mV/s. CPE is the unmodified electrode.

3. Results and discussion

3.1. Selection of the best electrode modifier

We have previously investigated MWCNTs-modified carbon paste electrodes for the direct electrochemical detection of living bacterial cells (Hassan et al., 2014). However, the assay sensitivity was not enough to detect the viable cell density below an OD_{600} of 0.1. Therefore, in this study, several nanomaterials were investigated as alternative electrode modifiers and NADH was used as a redox probe to evaluate the performance of each modified electrode. In this regards, NADH oxidation on electrode surface modified with nanomaterials such as Ag-NPs, Au-NPs, SWCNTs, MWCNTs, GO-AuNP and GO-Al_2O_3 composite was performed using cyclic voltammetry. As shown in Fig. 1, electrochemical responses of the nanostructured electrodes exhibited a significant enhancement in the oxidation of NADH with GO-Al_2O_3 exhibiting the highest oxidation current and the sharpest peak. Therefore, the GO-Al_2O_3 composite was selected as the electrode modifier and its physical and electrochemical characterizations were conducted.

3.2. Physical characterization

The morphology and size of the GO-Al_2O_3 nanocomposite particles were first examined using scanning electron microscopy (SEM) and transmission electron microscopy (TEM). As shown in Fig. 2a and b, the GO-Al_2O_3 particles exhibit a spherical morphology with particle sizes varying from 50–300 nm and an average size of ~200 nm consisting of GO sheet decorated with Al_2O_3 nanocrystals. To demonstrate the enhancement of the surface area of the GO-Al_2O_3 composite as compared to Al_2O_3, a SEM of the Al_2O_3 is shown in Fig. S1. The high surface area to volume ratio of the composite particles is attributed for the enhancement of the electrochemical activity of the nanocomposite and promoting the direct electron transfer at the electrode surface. The crystalline nature of the GO-Al_2O_3 nanocomposite was analyzed using

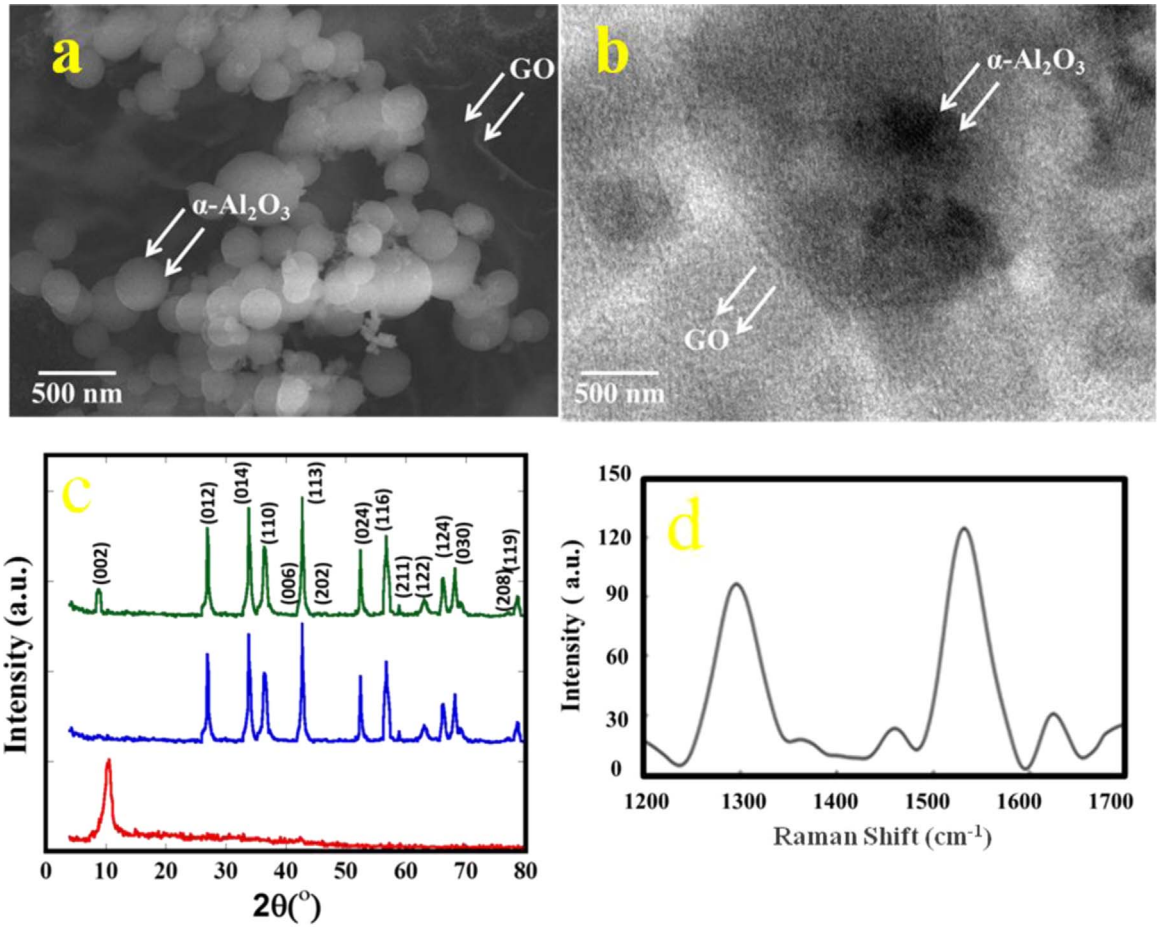

Fig. 2. a) Scanning electron microscope (SEM) images of GO/Al_2O_3 composite powder. The scale bar in (A) is 500 nm. b) Transmission electron microscope (TEM) images of GO/Al_2O_3 composite particles on a high resolution C-coated TEM grid showing the GO layers decorated with Al_2O_3 nanoparticles. c) XRD patterns of GO (red), α-Al_2O_3 (blue) and GO/Al_2O_3 nanocomposite (green). d) Raman spectra of the GO/ Al_2O_3 composite showing the characteristic graphitic peaks, D band ~1300 cm^{-1} and G band ~1560 cm^{-1}. (For interpretation of the references to color in this figure legend, the reader is referred to the web version of this article.)

X-ray diffraction (XRD). The XRD of the composite (green trace in Fig. 2c) reflects the formation of crystalline structure. Peaks at 26.7°, 33.7°, 36.4°, 40.6°, 42.7°, 45.5°, 52.4°, 56.8°, 58.8°, 62.7°, 66.0°, 68.2°, 77.1°, 78.4° which are corresponding to Miller indices (012), (014), (110), (006), (113), (202), (024), (116), (211), (122), (124), (030), (028) and (119), respectively, indicate the existence of a corundum hexagonal phase of the α-Al_2O_3 [32]. The broad peak appearing at 2θ=10.5° (d=0.85 nm) in pure GO and the composite corresponds to the Miller index (002) and is indicative of presence of GO.

The presence of graphitic nature of the graphene oxide (GO) sheets was also confirmed using Raman spectroscopy (Fig. 2d). The peaks characteristic to graphene oxide, namely D-band at 1300 cm^{-1} and G-band at 1560 cm^{-1}, were observed. The broad nature of G peak is indicative that the GO flakes are of multi-layer nature.

3.3. Electrochemical characterizations

The electrochemical performance of GO-Al_2O_3/CPE was characterized by performing cyclic voltammetry (CV) with $K_3[Fe(CN)_6]$ as the redox mediator. For comparison, the cyclic voltammograms of an unmodified CPE and CPE modified with individual components of the composite (Al_2O_3/CPE and GO/CPE) were analyzed. As shown in Fig. 3A, the Al_2O_3/CPE and GO/CPE showed higher electrochemical signal than the unmodified CPE. However, GO-Al_2O_3/CPE exhibited the best performance with peak currents (anodic and cathodic) an order of magnitude higher compared to unmodified CPE. This increase in peak current is indicative of enhancement of the electron transfer rate and electrocatalytic activity of the nanocomposite-modified electrode. We further analyzed two different concentrations of nanocomposite (10% and 50% by weight) for modification of CPE. As shown in Fig. 3B, upon increasing the composite concentration there was a significant increase in the electrochemical signal.

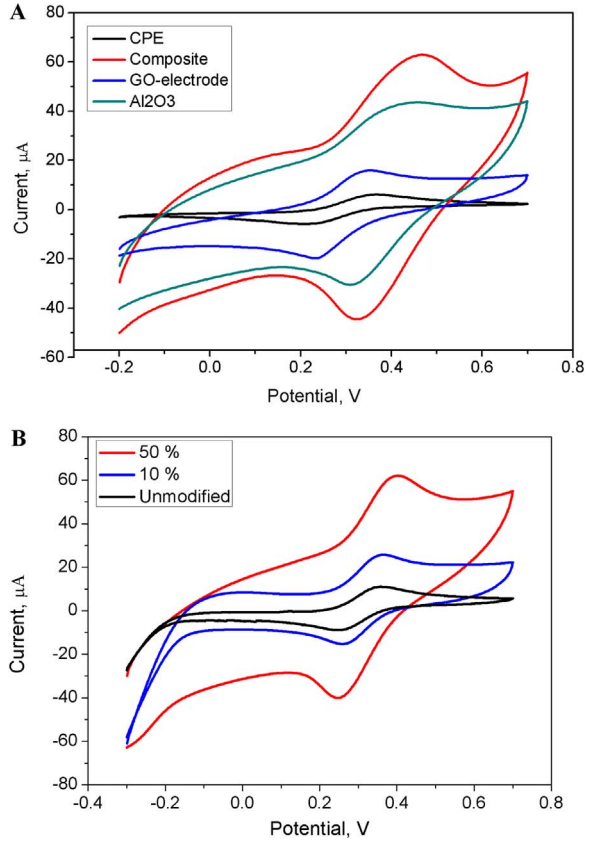

Fig. 3. A) Cyclic voltammograms for 0.1 mM $K_3[Fe(CN)_6]$ on GO, Al_2O_3 or GO/Al_2O_3 composite, at 40 mV/s in 0.1 M KCl. 3) Bioelectrochemistry of *E. coli* ($OD_{600\ nm}$ =0.5) using unmodified, GO, Al_2O_3 or GO/Al_2O_3 nanocomposite.

In addition to CV, electrochemical impedance spectroscopy (EIS) was used to determine the impact of the nanocomposite and its elements on the electrical conductivity of CPE. As shown in the Nyquist and Bode plots (Fig. S2 in Supplementary Information) the charge transfer resistance for the different electrodes were in the order of CPE > GO/CPE > Al_2O_3/CPE > GO- Al_2O_3/CPE. Further, the charge transfer resistance decreased with increasing concentration of the composite 50% GO- Al_2O_3/CPE < 10% GO- Al_2O_3/CPE; this is similar to the results obtained with CV. In particular, we observed the nanocomposite modified electrode fabricated using sonicated composite-graphite powder (before forming the paste) demonstrated even lower resistance (Fig. S2 in Supplementary Information). Based on the above results, 50% (by weight) GO-Al_2O_3 in synthetic carbon power was used for the fabrication of working electrode in subsequent experiments.

3.4. Metabolic pathway stimulation

The working cultures of bacterial cells were carefully washed with phosphate buffer to get rid of any electrochemically active or interfering chemical from the medium constituents or secreted metabolites from the overnight culture. The cell viability was determined by performing CV to measure the bioelectrochemical response of the metabolically active cells. As shown in Fig. 4A, on addition of aliquots of cell suspension containing 10 g/l of carbon sources to the electrolyte, an oxidation peak at a potential of ~0.76 V was observed. To confirm this oxidation peak corresponds to direct electrochemical activity of metabolically active cells, a control experiment was done where aliquots of the metabolically inactive cells with no carbon source were added to the phosphate buffer. The electrochemical response generated was much weaker compared to the response from metabolically active cells. Additionally, a negative control experiment where phosphate buffer containing 10 g/l of glucose was used as electrolyte showed no oxidation peak. Thus, confirming that the electrochemical signal is primarily originating from metabolically active bacterial cells.

We further investigated the effects of different carbon sources for the metabolic pathway stimulation. The metabolic pathway was then activated by adding glucose, acetate, sucrose, succinate, citrate or fructose to the phosphate buffer at a final concentration of 10 g/l. As illustrated in Fig. 4B, bacterial cells incubated with glucose, succinate or acetate as the carbon source exhibited higher anodic peak current values compared to cells incubated with other carbohydrates. Since incubation of cells with glucose generated the highest electrochemical signal, the concentration of glucose feed was optimized by incubating washed cells of *E. coli* and *S. cerevisiae* with different glucose concentrations (0, 5, 10, 15, 20 and 30 g/l). As illustrated in Fig. 4C, maximum oxidation currents for *S. cerevisiae* and *E. coli* suspensions were produced at 20 g/l and 10 g/l glucose, respectively, and the oxidation current was higher for *S. cerevisiae* than for *E. coli*.

3.5. Effects of pH and scan rate

From the above results we have established that the electrochemical signal observed is a result of the electrocatalytic activity of metabolically active microbial cells. Apart from the carbon feed source and their concentration, the influence of pH on bacterial cells viability is an important parameter. To determine the effect of pH, aliquots of metabolically active cells were added to phosphate buffer solutions from pH of 4–10 containing glucose (10 g/l) and the corresponding cyclic voltammograms were obtained. As shown in Fig. S3A, the oxidation current increased with increasing pH and reached a maximum value at pH 7.5, above this value the current started to decay. Therefore, pH 7.5 was chosen to be the optimal. In this experiment, the colorimetric measurement (WST-test) was used as a reference method.

In addition to the pH effect, scan rate is an important parameter that can influence the rate of electron transfer to the electrode surface

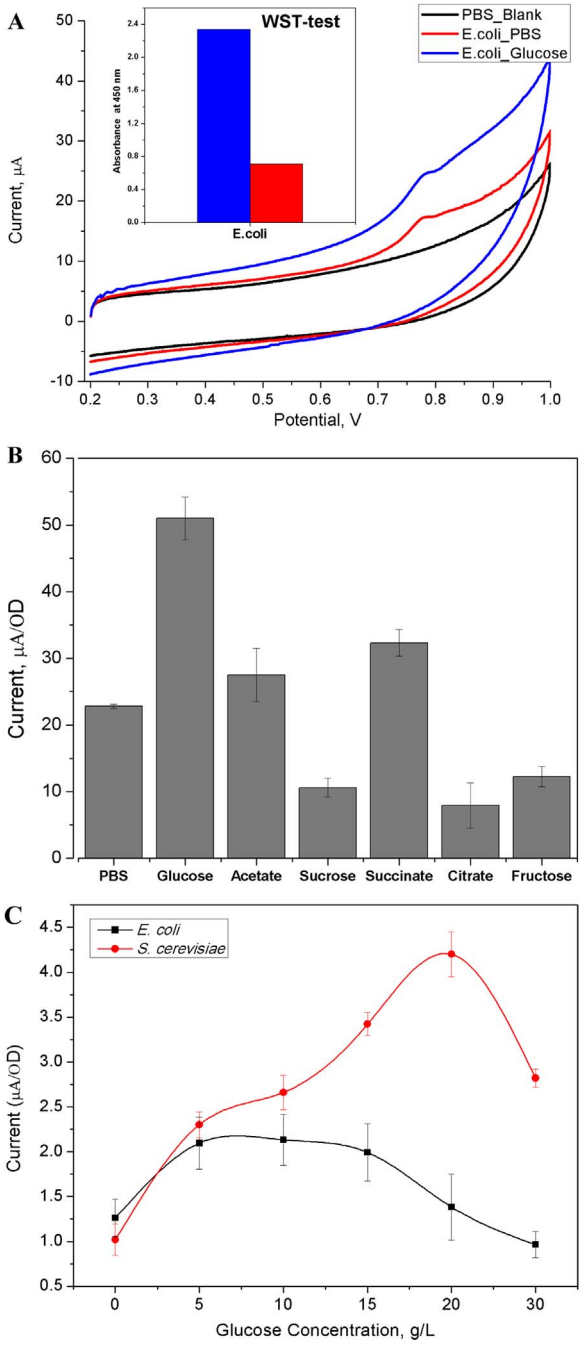

Fig. 4. (A) Bioelectrochemistry of metabolically active vs. metabolically inactive cells of *E. coli* with a comparison with the colorimetric responses of WST-test. (B) Effect of different carbon sources (10 g/l of each) on the oxidation current of *E. coli* (after 3 h of incubation). (C) Glucose concentration effect on the *E. coli* and *S. cerevisiae*.

and affect the sensitivity of detection. Fig. S3B shows the effects of obtained at scan rates varying from 5 to 300 mV/s, while keeping the other parameters constant. With increasing scan rate there was an increase in the oxidation peak current and a shift of peak potential to positive values. This observation proves that the electron transfer to electrode surface is diffusion controlled for the irreversibility of adsorbed redox species (Gowda and Nandibewoor, 2014; Prashanth et al., 2011).

3.6. Principle of detection

Fig. 5A shows the CVs of metabolically activated suspension of *E. coli* by 10g/l glucose and the same solution after the removal of cells by centrifugation (the supernatant). A similar magnitude of the anodic peak current for both indicates that the electrochemical response is emanating from metabolite(s) secreted by the cells and hence the principle of detection can be depicted by the schematic in Fig. 5B. However, no direct communication was found between the electrode surface and the living microbial cells, since the secreted metabolites behaved similar to the cell suspensions. Thus, the direct of oxidation of the secreted electrochemically active molecule(s) by the modified nanostructured electrodes is representing the simple direct detection of cell viability of metabolically active microbial cells.

3.7. Monitoring microbial density

Fig. 6 shows a plot of the peak anodic current of *E. coli* and *S. cerevisiae* after stimulation with carbon source and the density of cells at the time of stimulation (monitored as optical density). The results show a good correlation between the two parameters for both organisms, suggesting the capability of the proposed electrochemical activity measurement technique as a monitoring microbial density/concentration tool. Further, since this technique monitors the electroactive metabolites produced by the cells upon feeding a carbon source and therefore would be useful for monitoring viable cells sensitively and rapidly. The proposed method has advantages over the traditional microbiological and molecular methods that can either measure viable cells but require long time or unable to differentiate between viable and dead cells. The limit of detection in case of *E. coli* was determined to be 0.05 OD_{560}, which is suitable to detect the cell viability at this low cell concentration. However, in case of *S. cerevisiae*, the assay was comparatively less sensitive and lowest concentration detected was approximately 0.1 OD_{600}.

3.8. Antimicrobial susceptibility testing

Since the developed assay is capable of determining cell viability down to low cell concentrations, we further exploited our platform for screening the susceptibility of metabolically active *E. coli, B. subtilis, Enterococcus, P. aeruginosa and S. typhi* to ampicillin and kanamycin. The results showed (See Table S1, supplementary materials) *E. coli, B. subtilis* and *P. aeruginosa* were susceptible to both ampicillin and kanamycin, *Enterococcus* spp. was susceptible to kanamycin and resistive to ampicillin and *Salmonella* Spp. was resistant to both antibiotics. These results were in accordance with literature (Frech et al., 2003). Therefore, the developed

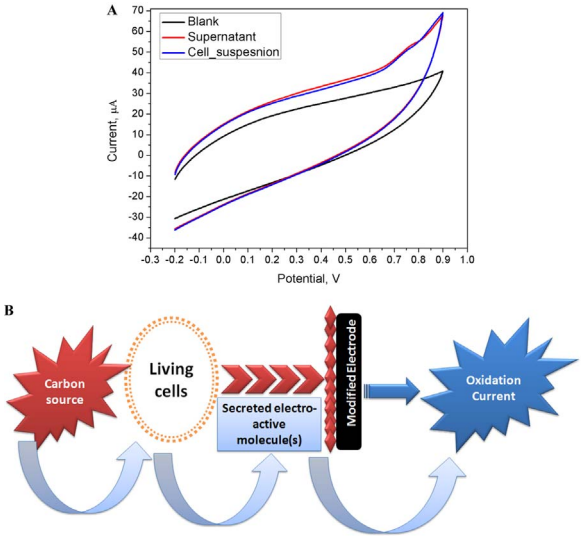

Fig. 5. The bioelectrochemical responses of cell suspension and supernatant after incubation for 3 h in glucose (A), description of the identified mechanism of the signal transfer from the metabolically active cells to the modified electrode surface (B).

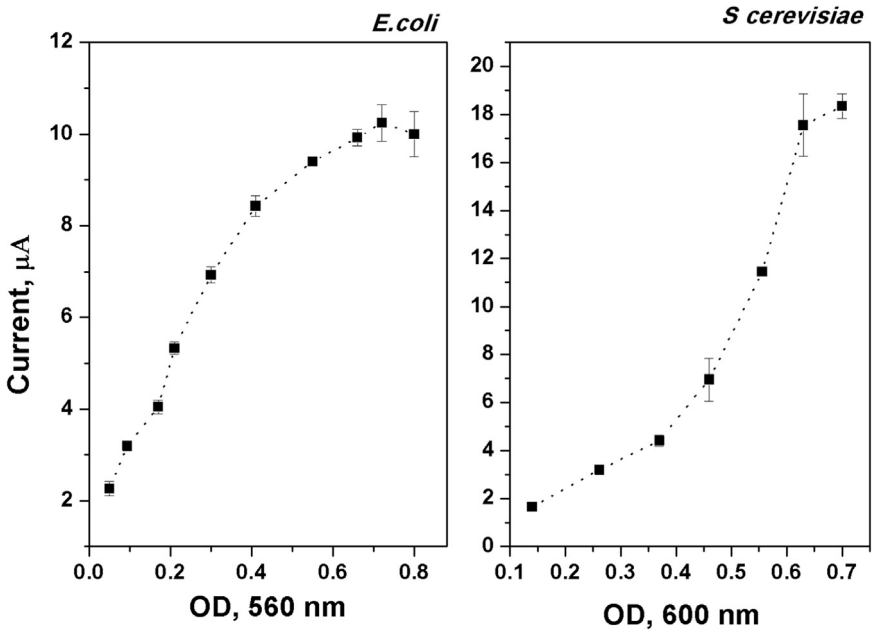

Fig. 6. Electrochemical monitoring of microbial cell density of *E. coli* and *S. cerevisiae*.

assay could be suitable for cell proliferation and cytotoxicity testing, since it monitors the live-cell functions under different growth conditions.

4. Conclusion

In the current study, we have developed a sensitive bioelectrochemical assay for measuring the cell viability of pathogenic microorganisms using a GO-Al_2O_3 nanocomposite. The nanocomposite was synthesized via physical mixing followed by characterization using several morphological and electrochemical techniques. The assay was optimized and the secreted soluble metabolites in the extracellular matrix were directly detected. The proposed method was successfully used for screening the susceptibility of metabolically active *E. coli, B. subtilis, Enterococcus, P. aeruginosa and S. typhi* to antibiotics. Thus, the GO-Al_2O_3 nanocomposite is a promising electrode modifier to provide a sensitive bioelectrochemical assay for measuring the cell viability of pathogenic microorganisms. Such combination is expected to have more applicability in the near future for sensitive and selective molecular recognitions and bioelectrochemical biosensors.

Acknowledgements

Authors acknowledge the financial support received from The Science and Technology Development Fund (STDF, Egypt) for funding the running research project (code 11929). AM acknowledges the financial support from W. Ruel Johnson Chair in Environmental Engineering.

Appendix A. Supporting information

Supplementary data associated with this article can be found in the online version at doi:10.1016/j.bios.2017.01.060.

References

Byrne, B., Stack, E., Gilmartin, N., O'Kennedy, R., 2009. Sensors 9 (6), 4407–4445.
Carmona-Martinez, A.A., Harnisch, F., Fitzgerald, L.A., Biffinger, J.C., Ringeisen, B.R., Schröder, U., 2011. Bioelectrochemistry 81 (2), 74–80.
Chalenko, Y., Shumyantseva, V., Ermolaeva, S., Archakov, A., 2012. Biosens. Bioelectron. 32 (1), 219–223.
Chen, S., Zhu, J., Wu, X., Han, Q., Wang, X., 2010. Graphene Oxide–MnO2 Nanocomposites for Supercapacitors. ACS. Nano. 4 (5), 2822–2830.
Esfandiari Baghbamidi, S., Beitollahi, H., Karimi-Maleh, H., Soltani-Nejad, S., Soltani-Nejad, V., Roodsaz, S., 2012. J. Anal. Methods Chem. 2012, 305872.
Frech, G., Kehrenberg, C., Schwarz, S., 2003. J. Antimicrob. Chemother. 51 (1), 180–182.
Gorby, Y.A., Yanina, S., McLean, J.S., Rosso, K.M., Moyles, D., Dohnalkova, A., Beveridge, T.J., Chang, I.S., Kim, B.H., Kim, K.S., Culley, D.E., Reed, S.B., Romine, M.F., Saffarini, D.A., Hill, E.A., Shi, L., Elias, D.A., Kennedy, D.W., Pinchuk, G., Watanabe, K., Ishii, S., Logan, B., Nealson, K.H., Fredrickson, J.K., 2006. Proc. Natl. Acad. Sci. USA 103 (30), 11358–11363.
Gowda, J.I., Nandibewoor, S.T., 2014. Asian J. Pharm. Sci. 9 (1), 42–49.
Hassan, R.Y., Bilitewski, U., 2011a. A viability assay for Candida albicans based on the electron transfer mediator 2,6-dichlorophenolindophenol. Anal. Biochem. 419 (1), 26–32.
Hassan, R.Y.A., Bilitewski, U., 2011b. Anal. Biochem. 419 (1), 26–32.
Hassan, R.Y.A., Bilitewski, U., 2013. Biosens. Bioelectron. 49, 192–198.
Hassan, R.Y.A., Hassan, H.N.A., Abdel-Aziz, M.S., Khaled, E., 2014. Sens. Actuators B: Chem. 203, 848–853.
Heiskanen, A., Coman, V., Kostesha, N., Sabourin, D., Haslett, N., Baronian, K., Gorton, L., Dufva, M., Emneus, J., 2013. Anal. Bioanal. Chem. 405 (11), 3847–3858.
Lim, D.V., Simpson, J.M., Kearns, E.A., Kramer, M.F., 2005. Clin. Microbiol. Rev. 18 (4), 583–607.
Logan, B.E., 2009. Nat. Rev. Microbiol. 7 (5), 375–381.
Marcano, D.C., Kosynkin, D.V., Berlin, J.M., Sinitskii, A., Sun, Z., Slesarev, A., Alemany, L.B., Lu, W., Tour, J.M., 2010. ACS Nano 4 (8), 4806–4814.
Marsili, E., Baron, D.B., Shikhare, I.D., Coursolle, D., Gralnick, J.A., Bond, D.R., 2008. Proc. Natl. Acad. Sci. USA 105 (10), 3968–3973.
Nishio, K., Nakamura, R., Lin, X., Konno, T., Ishihara, K., Nakanishi, S., Hashimoto, K., 2013. Chemphyschem.
Park, H.I., Sanchez, D., Cho, S.K., Yun, M., 2008. Environ. Sci. Technol. 42 (16), 6243–6249.
Prashanth, S.N., Ramesh, K.C., Seetharamappa, J., 2011. Int. J. Electrochem. 2011, 7.
Rabaey, K., Boon, N., Hofte, M., Verstraete, W., 2005. Environ. Sci. Technol. 39 (9), 3401–3408.
Reguera, G., McCarthy, K.D., Mehta, T., Nicoll, J.S., Tuominen, M.T., Lovley, D.R., 2005. Nature 435 (7045), 1098–1101.
Schroder, U., 2007. Phys. Chem. Chem. Phys. 9 (21), 2619–2629.
Spiegelman, D., Whissell, G., Greer, C.W., 2005. Can. J. Microbiol. 51 (5), 355–386.
Tian, B., Lieber, C.M., 2013. Annu. Rev. Anal. Chem. 6 (1), 31–51.
von Wintzingerode, F., Gobel, U.B., Stackebrandt, E., 1997. FEMS Microbiol. Rev. 21 (3), 213–229.
Wang, D., Choi, D., Li, J., Yang, Z., Nie, Z., Kou, R., Hu, D., Wang, C., Saraf, L.V., Zhang, J., Aksay, I.A., Liu, J., 2009. Self-Assembled TiO2–Graphene Hybrid Nanostructures for Enhanced Li-Ion Insertion. ACS. Nano. 3 (4), 907–914.
Yang, Y., Xu, M., Guo, J., Sun, G., 2012. Process Biochem. 47 (12), 1707–1714.
Yoon, S.M., Choi, C.H., Kim, M., Hyun, M.S., Shin, S.H., Yi, D.H., Kim, H.J., 2007. J. Microbiol Biotechnol. 17 (1), 110–115.
Yuan, Y., Ahmed, J., Zhou, L., Zhao, B., Kim, S., 2011. Biosens. Bioelectron. 27 (1), 106–112.
Zhao, H.Z., Du, Q., Li, Z.S., Yang, Q.Z., 2012. Sensors 12 (8), 10450–10462.